Academic Sciences International Journal of Pharmacy and Pharmaceutical Sciences

ISSN- 0975-1491 Vol 6 suppl 2, 2014

Research Article

INSIGHTS INTO THE STRUCTURAL AND FUNCTIONAL ASPECTS OF RELA BY MOLECULAR MODELING AND DOCKING CALCULATIONS

AMBILY NATH I.V, LOKA BHARATHI P. A, DEEPTI D. DEOBAGKAR*

Bioinformatics Centre, Biodiversity Informatics Group, BOD, National Institute of Oceanography, Goa, Coordinator, Biodiversity Informatics Group, BOD, National Institute of Oceanography, Goa, Director, Bioinformatics Centre & Professor, Department of Zoology, University of Pune, Maharashtra, India. Email: deepti.deobagkar@gmail.com

Received: 04 Dec, 2013 Revised and Accepted: 12 Feb, 2014

ABSTRACT

Objective: RelA (ppGpp synthetase I) has been reported as an excellent drug target due to its correlation with virulence induction in bacteria. The aim of present investigation is to provide a deeper understanding of the structural and functional aspects of RelA by an *in silico*-based approach.

Methods: Molecular models were proposed for the catalytic domain of RelA in two Gram negative bacteria *Pseudomonas aeruginosa* and *Vibrio vulnificus*, in former one, RelA contributes to virulence whereas no such data have published in the second case. These models were subjected to docking calculations using ppGpp synthetic analogues.

Results: The binding pocket characteristics in RelA are prone to fluctuations due to changes in some crucial interacting residues and this can have a profound influence on the binding interactions with ligands. GRxKH, a cationic motif, was observed to make consistent interactions with inhibitors, hence, suggested to have role in the charge transfer mechanism during signaling cascades.

Conclusion: These functional residues/motifs could be key determinants of pharmacological selectivity and specificity in RelA. At the same time, they also demand comprehensive experimental studies like site-directed mutagenesis to demonstrate their involvement in inducing virulence factors.

Keywords: RelA, *Psedomonas aeruginosa*, *Vibrio vulnificus*, Homology Model, ppGpp Synthetic Analogues, Docking, Key residues/motif

INTRODUCTION

The polyphosphate signal nucleotides pppGpp (guanosine 3'-diphosphate 5'-triphosphate) and ppGpp (guanosine 3', 5'-bisdiphosphate) (collectively termed as (p)ppGpp) [1-4] play pivotal roles in bacterial defense mechanism such as stringent response. (p)ppGpp is modulated by the coordinated action of two protein kinases- RelA and SpoT, members of RSH (RelA SpoT Homologue) superfamily [5-7]. Generally known as GTP/GDP pyrophosphokinases (EC 2.7.6.5), RelA and SpoT enzymes catalyze the transfer of a pyrophosphate (PPi) from ATP (adenosine triphosphate) to GTP/GDP while the subsequent reversal of the process is carried out by SpoT [8-11].

Although paralogous in nature, functionally RelA and SpoT are different. RelA ((p)ppGpp synthetase I) is the 84 kDa ribosome-associated protein and carries out the synthesis of (p)ppGpp [12-15]. The 79 kDa SpoT ((p)ppGpp synthetase II) is a cytosolic bifunctional enzyme which catalyze both synthesis and hydrolysis of (p)ppGpp [8, 16, 11, 6]. The systematic and programmed expression of RelA and SpoT together regulate the (p)ppGpp biosynthesis pathway in Gram negative bacteria [11, 17-19].

The molecular architecture of SpoT and RelA is characterized by a catalytic N-terminus and a regulatory C-terminus (Battesti and Bouveret 2006). In SpoT, the N-terminus possesses two domains namely- HD (hydrolase) and SD (synthetase) [6, 11]. The functional relevance of HDxxED and RxKD motifs in the HD and SD of SpoT has already been reported [8]. In RelA, HD domain is shown to be inactive [6, 11, 14] and RxKD is replaced by an ExDD [16]. Mutagenesis studies have demonstrated that RxKD and ExDD motifs are instrumental in determining the Mg^{2+}-dependent inhibitory effect on (p)ppGpp synthesis as well as in substrate (GDP/GTP) specificity [8]. The site-directed mutagenesis conducted by Gropp et al. [20] has revealed that Gly251 and His354 in the N-terminus are essential for the enzymatic activity of RelA in *Escherichia coli*. The C-terminus of SpoT and RelA is composed of ACT (derived from Aspartokinase, Chorismate mutase, Tyr A) [21] and TGS (named after the Threonyl-tRNA synthetase (ThrRS), GTPase, and SpoT/RelA proteins where it occurs) domains [22, 23, 14, 11].

The expression of RelA and SpoT has been correlated with virulence in many pathogenic bacteria such as *Mycobacterium tuberculosis* [24, 25], *Listeria monocytogenes* [26], *Legionella pneumophila* [27, 28], *Vibrio cholerae* [29], *Pseudomonas aeruginosa* [30, 31], *Yersinia pestis* [32], *Burkholderia pseudomallei* [33], *Salmonella enterica* serovar Typhimurium [34], *Francisella novicida* [35] and *Enterococcus faecalis* [7]. In *Escherichia coli* [36, 37] and *Vibrio vulnificus* [38], ppGpp plays a crucial indirect role as it positively regulates RpoS (a stress factor as well as virulence factor) synthesis [11]. Hence, from a therapeutic perspective, RelA and SpoT have been reported as excellent drug targets [31, 1, 39, 40]. The pathogenic potential of RelA was observed to be particularly more pronounced than SpoT.

The development of novel antibacterial compounds as competitive inhibitors of Rel (alternatively RSH) proteins is an active research area. Recently, Wexselblatt et al. [41, 42] have published a series of ppGpp synthetic analogues with promising antibacterial activity towards Rel and RelA. They also modeled the binding interactions between the most potent analogue and experimental structure of Rel_{seq}, another member of RSH superfamily. Since the crystallization of membrane proteins is extremely difficult, to date, no experimentally determined structure is available for the functional homologue of Rel, RelA.

In order to get further insights into the structural and functional aspects, the present study has proposed molecular models for the catalytic domain (1-385 residues) of RelA in Gram negative bacteria *P.aeruginosa* (Model P) and *V.vulnificus* (Model V) by homology modeling. The A chain of RSH from *Streptococcus equisimilis* (PDB: 1VJ7A) was selected as the template scaffold. The generated models were subjected to docking simulations with ppGpp synthetic analogues; the binding interactions were characterized and analyzed with respect to structural differences in models. The results were crosschecked with experimental observations. This *in silico* model-integrated docking study could serve as a good platform for the clustering of functional motifs or hot spot residues in the binding pocket of RelA. Such potential druggable regions could be harnessed for the design of RelA-specific antibacterial compounds. These results could also be employed for structure-based pharmacophore modeling and in site-directed mutagenesis experiments.

MATERIALS AND METHODS

Construction of 3D Model

The target RelA sequences of *P.aeruginosa* (RelAp, Accession: NP_249625) and *V.vulnificus* (Relv, Accession: NP_935614) were accessed from NCBI (www.ncbi.nlm.nih.gov) and only the catalytic domain portion (1-385 residues) was considered for the study. The PSI-BLAST algorithm [43] has identified the 2.1Å X-ray crystal structure of 1VJ7A possessing the conformation –(p)ppGpp hydrolase OFF/(p)ppGpp synthetase ON [40], as the best template from Protein Data Bank (PDB) (www.pdb.org). The target-template alignments were carried out in DeepView of Swiss PDB Viewer (SPDBV) 4.04. The 3D generation of the structural coordinates of the targets was performed by Swiss Model (http://www.swissmodel.expasy.org) web services using the optimize (Project mode) mode. In order to stabilize the distorted geometry an energy minimization of the models was accomplished in vacuo by GROMOS96 force field implemented in SPDBV [44]. The stereochemical quality of the refined structures was evaluated by Profunc PROCHECK [45] and ProSA Z-score [46] programs.

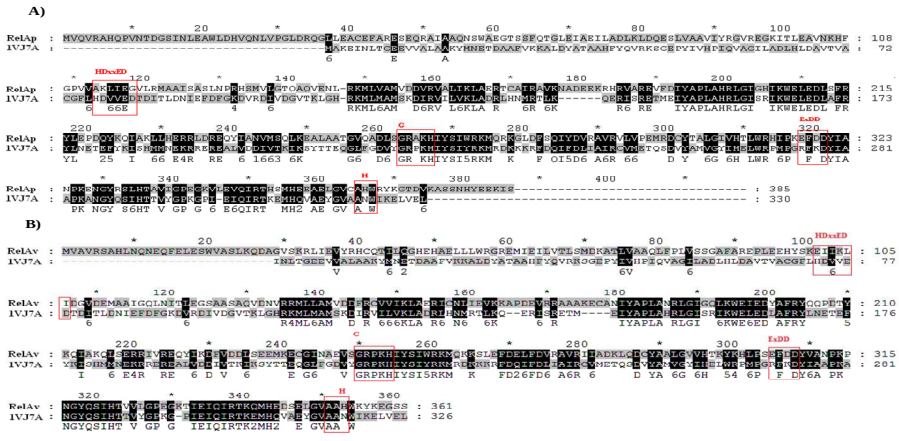

Fig. 1: Sequence alignment of RelA sequences with 1VJ7A. A) RelAp-1VJ7A B) RelAv-1VJ7A. The identical and similar residues are shaded in black boxes. Red framed boxes denote functional motifs (HDxxED, RxKD/ExDD) and residues (Gly of GRPKH and His of AAH). The alignment is visualized in GeneDoc2.7 [51].

Electrostatic Potential Analysis

The electrostatic charge distribution in the models was calculated by the Adaptive Poisson-Boltzmann Solver (APBS) program [47]. A comparative analysis of the difference in electrostatic potential of the hypothetical structures has been carried out. PyMOL (academic version) (www.pymol.org) was utilized for the visualization of surface representation.

Selection of Ligands

The putative models were subjected to docking calculations using ppGpp synthetic analogues reported by Wexselblatt et al. [41, 42]. These guanosine derivatives having substituent at 3' and 5' positions of ribose showed good inhibitory activity against RelA. Hence, we used these compounds in the present simulation (since being a metal coordinate compound 5d was omitted from the dataset)

.

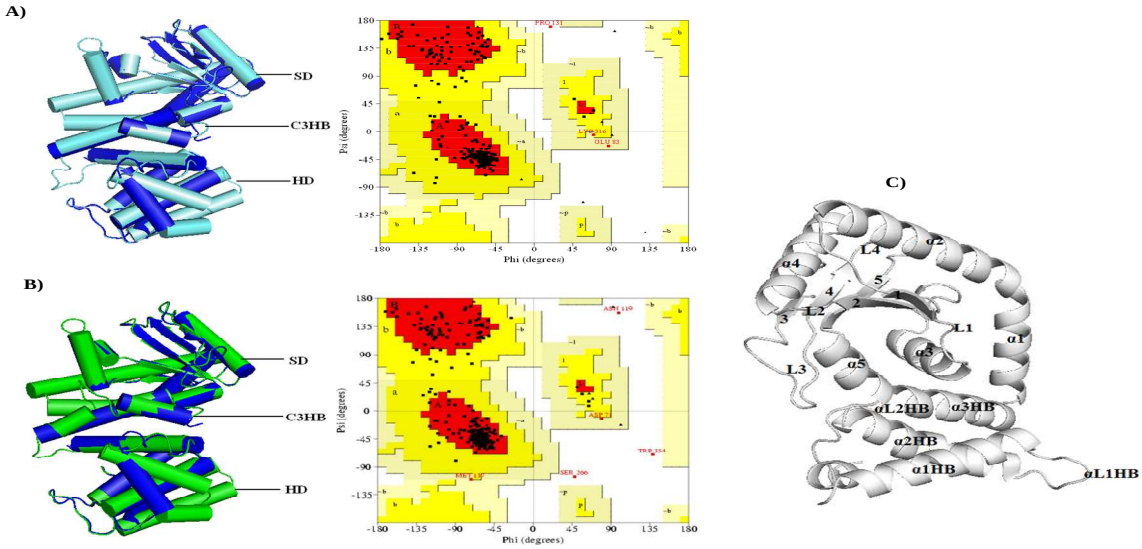

Fig. 2: Superimposition of template (blue) with 3D models and PROCHECK results. A) Model P (cyan) B) Model V (green). C) The secondary structural components of SD and associated C3HB linker are visualized. The helices, strands and loops of SD are marked as α1-α5, 1-5 and L1-L4 respectively whereas inC3HB, the helices and loops are denoted as α1HB, αL1HB, α2HB, αL2HB and α3HB respectively.

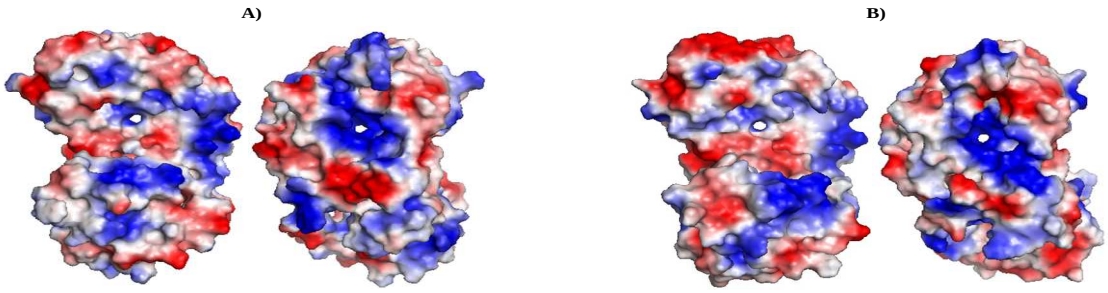

Fig. 3: Electrostatic charge distribution. Front and back view of models showing pore of the substrate binding pocket. Blue, red and white represent positive, negative and neutral charge potential. A) Model P B) Model V.

Molecular Docking

AutoDock 4.0 and its graphical user interface AutoDock Tools (ADT) 1.5.4 [48] were used to set up the protein and ligand files for docking. The polar hydrogen and Kollman charges were added to the theoretical protein models. All ligands were sketched using Marvin Sketch 5.3.4 (ChemAxon) software. ADT initialized the ligands with the merging of non-polar hydrogen and addition of Gasteiger charges. In docking, the protein was considered as a rigid body while treating the ligand as a flexible compound. AutoTors was used to identify the rotatable bonds in ligands. AutoGrid calculated the binding pockets of protein by the creation of potential interaction grid boxes. The binding pocket details were extracted from the co-crystalized ligand GDP. Grid boxes with dimension of 40*40*40 (grid spacing 1.000Å) which cover the binding pocket were used for simulation in models using an exhaustiveness option of 50. The ligands were docked into the substrate binding pockets of Models P and V by AutoDock Vina (also referred to as Vina) [49].

The docking graphics was visualized through PyMOL.

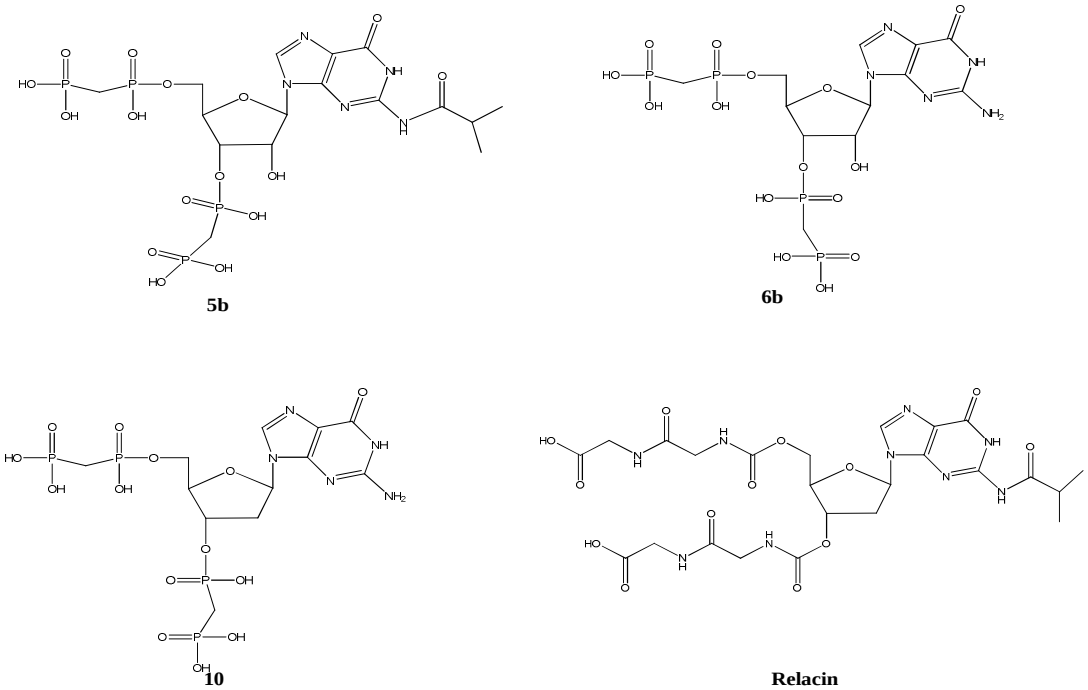

Fig. 4: ppGpp synthetic analogues with methylene bisphosphonates (5b, 6b and 10) and glycineglycyl dipeptieds (relacin) at 3', 5' positions of guanosine.

RESULTS AND DISCUSSION

In microbes, ppGpp is instrumental in controlling the signaling cascades in stringent response. RelA-mediated synthesis of this signal alarmone is also implicated in bacterial virulence and antibiotic resistance; hence, from a pharmacological perspective, RelA has been proposed as an excellent drug target for the discovery of novel compounds with desirable antibacterial properties and studies in this direction are progressing. At present, no experimentally solved 3D structure is available for RelA. This was the motivation for us to conduct the present investigation. We built the hypothetical model of RelA in two Gram negative bacteria- *P.aeruginosa* and *V.vulnificus*, in the former one, RelA induces virulence characteristics while no such direct role has been reported in the latter case. These putative models were subjected to docking simulations with ppGpp analogues to derive plausible binding modes and key residue interactions.

.

Generation of Structural Coordinates for RelA

In our study, we first modeled the catalytic domain of RelA using the structural coordinates of 1VJ7A. RelAp and RelAv shared 42% and 39% residue identities with template structure respectively (Figure 1). The sequence alignments were subjected to a careful visual scan to check the conservation status of functional motifs and key residues.

The SD which occupies the binding pocket was highly conserved in both cases. As already mentioned in the introduction section, it was not surprising that the HDxxED in bifunctional template showed least identity to the monofunctional RelA targets. In addition, RxKD in 1VJ7A was replaced by ExDD in RelA. Gly251 and His354 were conserved in the query sequences whereas poor electron density in the template masked the structural organization of His354

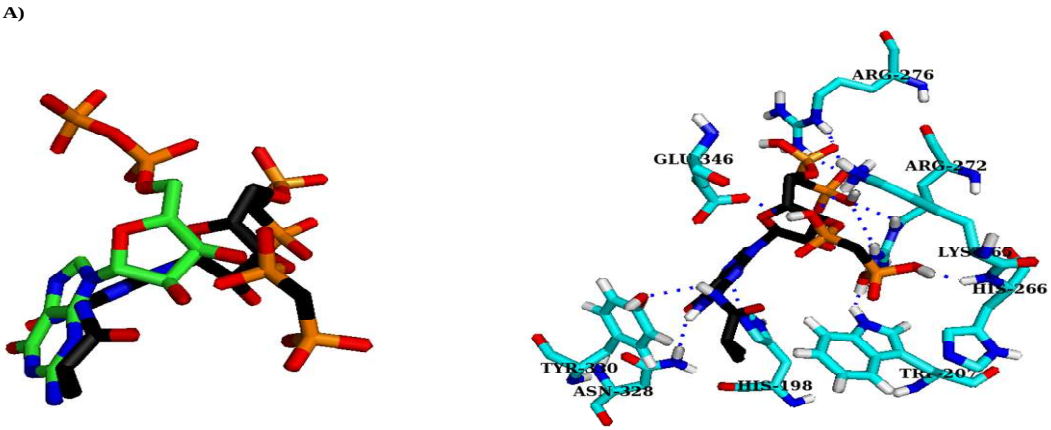

Fig. 5: Superimposition of the best docked pose (black) of analogue with bioactive conformation of GDP (green) and H-bonding interactions in the docked complex of analogues and Model P (cyan) are given. Nitrogen, phosphorus and hydrogen are colored in blue, orange and white respectively. H-bonds are shown as blue dashed lines. A) 5b B) 6b C) 10 D) Relacin.

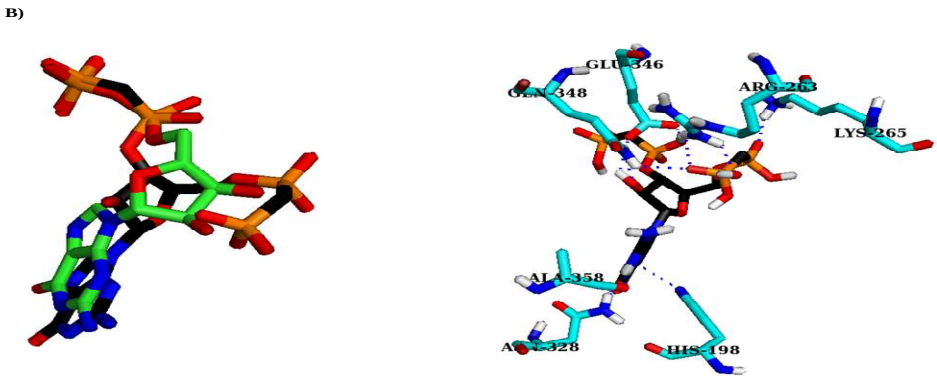

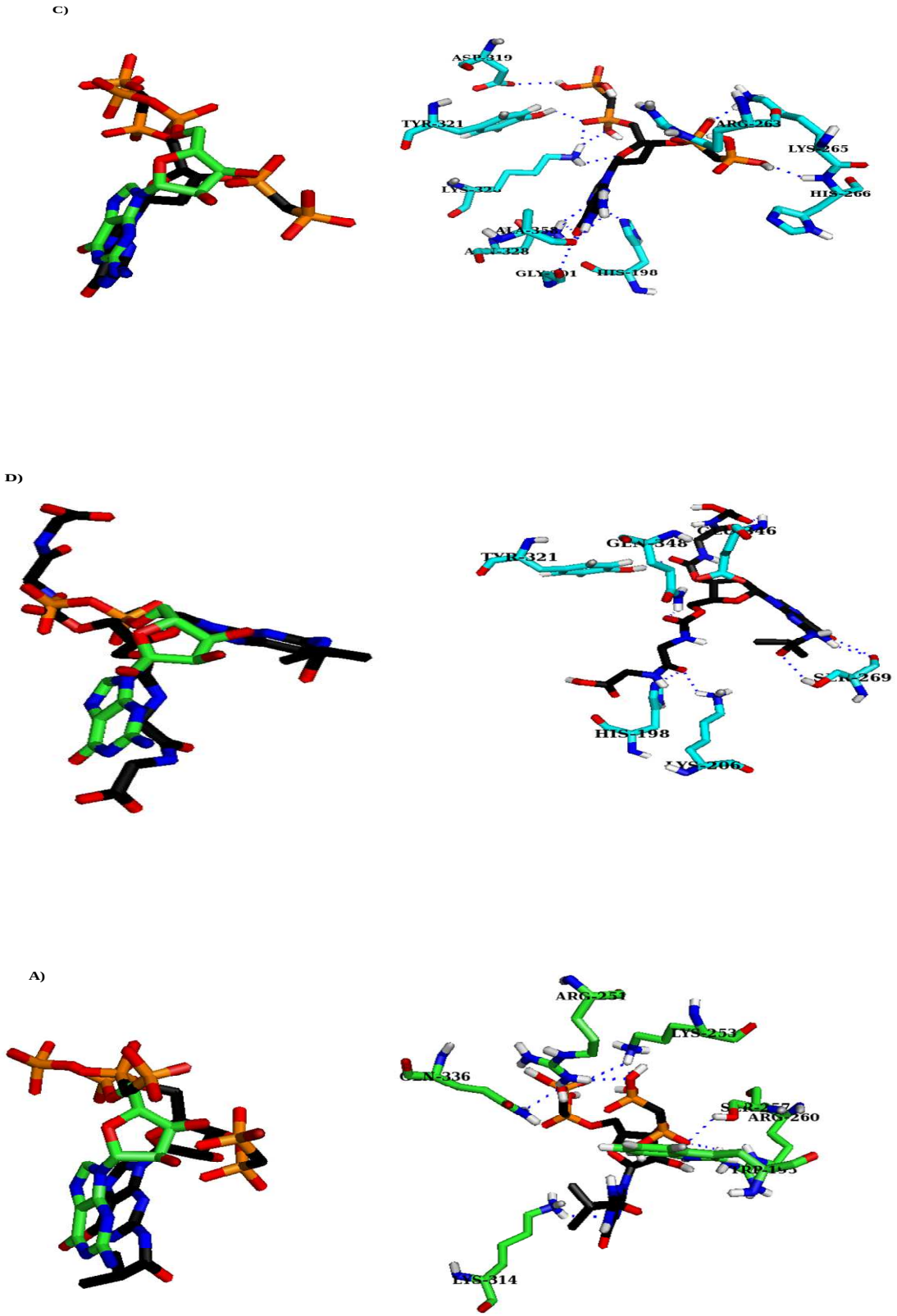

Fig. 6: Superimposition of the best docked pose (black) of analogue with bioactive conformation of GDP (green) and H-bonding interactions in the docked complex of analogues and Model V (green) are shown. A) 5b B) 6b C) 10 D) Relacin.

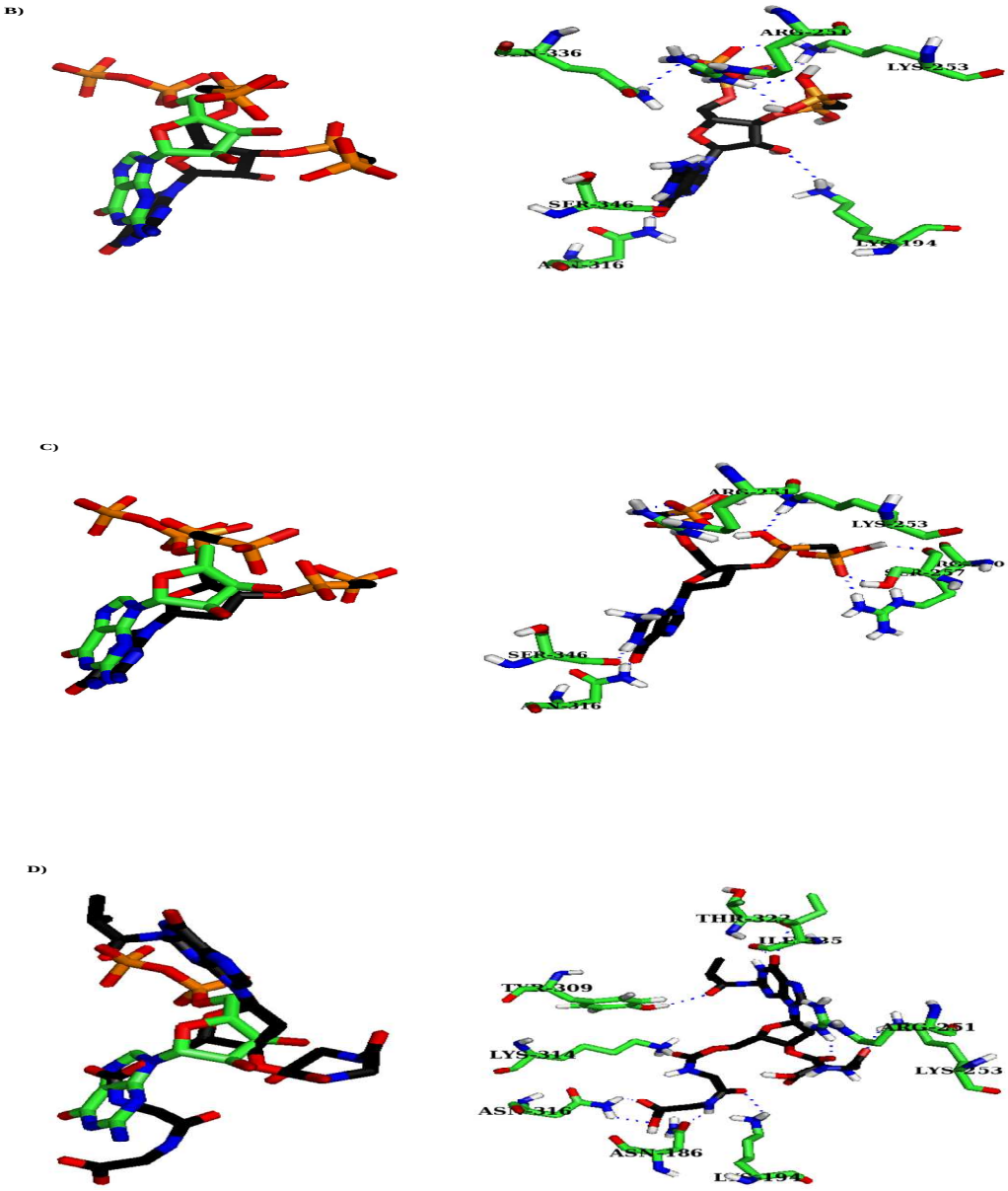

After energy minimization *in vacuo* the models were superimposed to the template structure and derived root mean square deviations (RMSDs) of 0.24 and 0.23Å for Models P and V respectively; this denotes that the backbone conformation of models is close to experimental structure (Figure 2). The stereochemistry of the models was evaluated by PROCHECK program. Models P and V possessed 91.2 and 89.5% residues in most favored; 8.2 and 8.8% residues in additionally allowed; 0.7 and 0.7% residues in generously allowed and 0.0 and 1.0% residues falling in disallowed regions respectively. The G-factors which assess the quality of the dihedrals, covalent and overall quality of the bond angles were -0.13, 0.20 and 0.00 for Model P; -0.15, 0.10 and -0.04 for Model V respectively. The ProSA Z-score of Model P was measured to be -5.39 and for Model V the score was -5.03. The structure assessment programs testified that all values were within the permitted limit of the putative models.

Salient Features of the Models

Both models recreated the basic topology of the experimental structure, that is, α-helix predominant N-terminal HD, central 3-helix bundle (C3HB) linker which connects N- and C-termini together, SD-occupied C-terminus with 5-stranded mixed β-sheet surrounded by 5 α-helices assembled together by hydrophilic loops. In this study, our interest was focused on the binding pocket-enclosed SD which was well characterized in both models. A comparative analysis of the binding pocket geometry in the models was carried out with template to monitor the conservation of functional residues. In 1VJ7A, Ser181, Arg241, Lys297, Tyr299, Lys304, Asn306, His312, Gln325 and Ala335 constitute the binding pocket. Model P showed two alterations from this- Ser181 was replaced by Gly203 and Lys297 was replaced by Asp319 whereas Model V possessed three replacements- Ser181 by Gly191, Lys297 by Asp307 and Ala335 by Ser346. In structure-based drug design, charge complimentarity between the binding pocket of the protein and ligand is an important aspect. Hence, in the present study, both protein models were directed to mapping of electrostatic charges onto the molecular surfaces and compared the nature of charge distribution (Figure 3). Interestingly, RelA in two Gram negative bacteria showed similarity as well as differences in surface potential dissemination. Model P showed an overall positive potential. Negative charge distribution was observed in Model V, the substituted polar negatively charged binding site residues also contribute towards this. The binding cavity in both cases was surrounded by a rich

positive potential with the distribution of arginine, lysine and histidine. Such an environment facilitates the binding of negatively charged compounds.

Docking Calculations with ppGpp Analogues

In order to shed light on the binding modes between RelA and antibacterial compounds, a docking simulation was performed on RelA 3D models using ppGpp synthetic analogues- 5b, 6b, 10 and relacin (Figure 4). These synthetic guanosine derivatives differed from ppGpp in certain features. Compounds 5b and relacin possessed substitutions at N2 nitrogen of guanine base. The 2'-hydroxyl was replaced by hydrogen atom in 10 and relacin. All compounds possessed substituent at 3' and 5' positions- the methylene bisphosphonate groups occupied both positions in 5b, 6b and 10 whereas glycyl glycine dipeptide was the substituent in relacin. Vina program was employed for docking. A total of 9 docking runs per compound were carried out. Of the maximum limit of 32 rotatable bonds, Vina has identified 20, 18, 17 and 23 active bonds for 5b, 6b, 10 and relacin respectively. To select a functionally relevant pose, predicted binding orientations similar to the experimental binding pose of GDP was chosen. In addition, good binding affinity and RMSD were also taken into consideration.

Mapping of Protein-Ligand Interactions

In Model P, the highest scored poses of 5b, 6b and 10 resembled the bioactive conformation of GDP- the guanine nucleotide was directed towards the hydrophilic interaction sites in βL3 and proximal α3 whereas the sugar and phosphate groups were poised by interactions from the stranded β sheets and interspersed loops. Relacin adopted an extended conformation with the purine ring poised by α3; the 3'-bisphosphonate was strengthened by residues from β5 and βL3 and 5'-bisphoaphonate was anchored by distal region of α2HB and proximal part of α3HB. The binding affinity and H-bonding residues of the best ranked pose of each analogue is provided in Table 1. A superimposed view of these compounds with GDP and the binding interactions are shown in Figure 5.

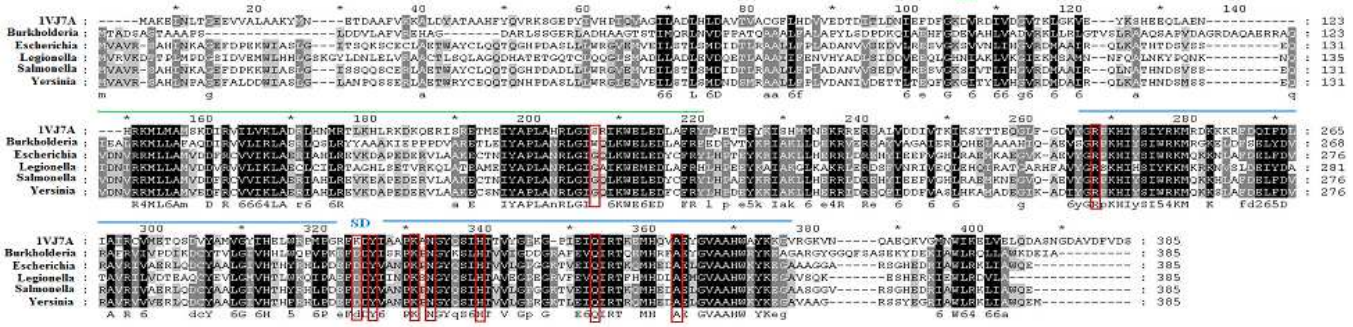

Fig. 7: Multiple sequence alignment of the catalytic domains of 1VJ7A and RelA sequences of *Burkholderia pseudomallei* K96243 (Burkholderia), *Escherichia coli* str. K12 sub str. W3110 (Escherichia), *Legionella pneumophila* subsp. pneumophila ATCC 43290 (Legionella), *Salmonella enterica* subsp. enterica serovar Typhimurium str. LT2 (Salmonella) and *Yersinia pestis* KIM10+ (Yersinia) visualized in GeneDoc. The nucleotide binding residues are tabulated in red column. HD and SD are marked in green and blue straight lines respectively.

Table 1: Docking Summary in Model P

Analogue	Binding Affinity (kcal/mol)	H-bonding Residues
5b	-7.6	His198, Asn328, Tyr330, Glu346, Lys265, His266, Arg272, Arg276, Trp207
6b	-7.8	His198, Arg263, Lys265, Asn328, Glu346, Gln348, Ala358
10	-7.2	His198, Gly201, Arg263, Lys265, His266, Asp319, Tyr321, Lys326, Asn328, Ala358
Relacin	-7.3	His198, Lys206, Ser269, Tyr321, Glu346, Gln348

Table 2: Docking Summary in Model V

Analogue	Binding Affinity (kcal/mol)	H-bonding Residues
5b	-7.1	Trp195, Arg251, Lys253, Ser257, Arg260, Lys314, Gln336
6b	-7.6	Lys194, Arg251, Lys253, Asn316, Gln336, Ser346
10	-7.8	Arg251, Lys253, Ser257, Arg260, Asn316, Ser346
Relacin	-7.4	Asn186, Lys194, Arg251, Lys253, Tyr309, Lys314, Asn316, Thr323, Ile335

The guanine scaffold in 5b, 6b and 10 formed extensive hydrogen bonds with polar residues such as His198, Gly201, Lys326, Asn328, Ty330, Glu346, Gln348 and Ala358. In 5b, superimposition with GDP showed that the predicted pose tilted a little, possibly due to the orientation of the aliphatic substituent at N2 of guanine towards the hydrophobic environment provided by Trp207, Ala358 and alkyl groups of Glu359. In all three cases, the 3' and 5' bisphosphonates were buried deep into the pocket and predominantly formed contacts with cationic residues. The binding orientation of 3'-bisphosphonate was in the opposite direction of the 5'-diphosphate

of GDP. Trp207, Arg263, Lys265, His266, Arg272, Arg276, Asp319, Tyr321, Lys326, Glu346 and Gln348 were the main interacting residues of phosphate groups. Relacin, with its stretched peptide arms was anchored by both hydrophilic (His198, Lys206, Gln348, Tyr321, Glu346) and hydrophobic (Trp207, Ile202, Glu360, Ala358, Leu360, methyl group of Thr335, Ala336, Val337, Glu317) interactions. Superimposition with GDP demonstrated that the 3'-substituent displayed the same orientation as the phosphate tail of GDP whereas the 5'-bisphosphonate group was oriented in the same direction as guanosine.

In Model V, all except relacin mimicked the binding conformation of GDP. In 5b, the N2 substituent of guanine showed hydrophobic interactions with Ile190, Trp195, Glu347 and Leu348. One H-bond from Lys314 also supported the nucleotide. As in the previous docking study, the bisphosphonates of 5b, 6b and 10 were surrounded by positively charged polar residues such as Lys194, Trp195, Arg251, Lys253, Ser257, Arg260 and Gln336. The guanine in 6b and 10 was anchored by H-bonds from Asn316 and Ser346 respectively. In a striking contrast to Model P, relacin adopted somewhat 'shrinked' conformation, particularly, the 3' bisphosphonate was observed to repel from the protein core. The ligand was bounded by hydrophobic (Ala185, Leu188, Ile190, Trp195, Pro252, Ile258, Phe306, Asp307, Asp308 and Leu348) and H-bonding (Asn186, Lys194, Arg251, Lys253, Tyr309, Lys314, Asn316, Thr323 and Ile335) interactions (Table 2 and Figure 6).

The docking results were compared with the experimental inhibitory properties of the analogues against RelA. The *in vitro* studies [41] demonstrated that 6b and 10 were dominant over others. Our results were in reasonable agreement with experimental data; however, it differed in two RelA models. In Model P, the highest binding affinity was shown by 6b followed by 5b. The dock scores of 10 and relacin were almost identical. Analogue 10 was dominant over others in Model V, remaining compounds descended in this order 6b> relacin >5b. In general, the N2 substituent had a negative effect on the docking performance as it is obvious from the lower scores of 5b and relacin. The 2'-OH and its replacement by H found to increase the hydrophilicity of the interactions. Contrary to our expectations that a polar positively charged binding pocket can well-accommodate a compound like relacin possessing hydrophilic groups, the peptide arms found to make steric clashes with the walls of the pocket and failed to adopt a stable conformation. This observation strongly supported the electrostatic potential analysis that negatively charged compounds can be good drug candidates.

Identification of Key residues/Functional Motifs

In drug-target interactions, key functional residues in the binding pocket of the protein play a crucial role in determining the pharmacological specificity and selectivity. As already discussed, while analyzing the degree of conservation of binding site residues, we found some differences in our RelA models with respect to those in template- in Model P, Ser181 and Lys297 (residue position denotes that in the template) were replaced by Gly203 and Asp319 respectively whereas in Model V, three residue changes were observed viz Ser181 by Gly191, Lys297 by Asp307 and Ala335 by Ser346. In order to check the restoration of key interacting residues in other genera of Gram negative bacteria we performed a multiple sequence alignment of the catalytic domains of RelA in *Burkholderia* (Accession: YP_108545), *Escherichia* (Accession: BAE76858), *Legionella* (Accession: YP_005185759), *Salmonella* (Accession: AAL21836) and *Yersinia* (Accession: NP_668147) with 1VJ7A (Figure 7). Ser181 in HD found to be highly varied and this could be correlated to the structural flexibility of the domain. Among Arg241, Lys297, Tyr299, Lys304, Asn306, His312, Gln325 and Ala335 in SD, only Lys297 showed alteration and it was replaced by an acidic aspartic acid. The binding pocket geometry of Model P was identical to all analyzed RelA sequences except *B.pseudomallei* whereas Model V sequence undergone the greatest variations. These results clearly demonstrate that the binding pocket characteristics in RelA are prone to fluctuations due to changes in some crucial interacting residues and it can have a profound influence on the binding interactions with ligands.

Next, we analyzed whether any residues are involved in frequent interactions and the replaced residues display any crucial role. It is observed that residues of a particular stretch, GRPKH (from here onwards we refer to this as GRxKH motif) form dominant consistent interactions with ligands, particularly, Arg263-Lys265 in Model P and Arg251-Lys253 in Model V respectively. It was also interesting to note that the functional significance of Gly201 which is one member of this motif was already proven experimentally [20]. Since the binding pocket is predominantly positively charged it could be possible that this cationic motif might be involved in some kind of charge transfer mechanism and promote the signaling process. Further site-directed mutagenesis studies are needed to confirm its biological role. In addition, we scrutinized the binding modes of all compounds to check the involvement of substituted key residues. In Model P docking, Gly203 was not involved in any interaction, but Asp319 observed to form an H-bond in compound 10. In the second docking trial with Model V, Ser346 was found to establish H-bond interactions with 6b and 10. From a pharmacological perspective, alterations in binding site residues can change the nature of binding pocket, for example, it can change the hydrophilic site to hydrophobic or vice versa. Such key factors should be taken into consideration while attempting a structure-based drug designing of novel inhibitors for RelA.

RelA, the enzyme which initiates the biochemical events in stringent response is correlated with virulence expression in many bacterial genera like *Pseudomonas*, *Legionella* and *Listeria*. However, no such reports have established in *V.vulnificus*, a pathogenic species, though RelA expression is confirmed in the stringent behavior [50]. The present *in silico* study demonstrated that some notable substitutions do exist in the substrate binding pocket residues of *V.vulnificus* bacterium. Such key residues might have crucial roles in interacting with natural substrates like GDP/GTP and in conferring virulence capabilities to the bacterial cell. In-depth studies in this direction could unravel such unanswered dilemmas.

CONCLUSION

The present investigation has employed an *in silico* approach for the structural characterization of RelA in two Gram negative bacteria. We firstly built the 3D models of the catalytic domain of RelA in *P.aeruginosa* (Model P) and *V.vulnificus* (Model V) based on the atomic coordinates of 1VJ7A as the structural template. A detailed docking simulation was carried out in each model using ppGpp synthetic analogues and the results were analyzed with respect to geometrical differences in the binding pocket of the models. Another characteristic feature deduced from the study was GRxKH, a cationic signature motif, and was observed to make consistent interactions with inhibitors, hence, suggested to have a role in the charge transfer mechanism during signaling process. Concluding our study, such residues/motif could be key determinants of pharmacological selectivity and specificity in RelA, at the same time; they also demand further comprehensive experimental studies to correlate their involvement in inducing virulence factors.

ACKNOWLEDGEMENT

We thank Director, NIO, for providing us the facilities to carry out the present work.

Abbreviation

EC- Enzyme Commission code

pppGpp- guanosine 3'-diphosphate 5'-triphosphate

ppGpp- guanosine 3',5'-bisdiphosphate

SpoT- ppGpp synthetase II

RelA- ppGpp synthetase I

RSH- RelA SpoT Homologue

RMSD- Root Mean Square Deviation

GTP/GDP- guanosine triphosphate/guanosine diphosphate

PPi- pyrophosphate

ATP- adenosine triphosphate

HD- hydrolase domain

SD- synthetase domain

ACT- aspartokinase, chorismate mutase, Tyr A

TGS- Threonyl-tRNA synthetase (ThrRS), GTPase and SpoT/RelA

REFERENCES

1. Chatterji D and Ojha AK. Revisiting the stringent response, ppGpp and starvation signaling. Curr. Opin. Microbiol. 2001; 4(2): 160-165.
2. Wendrich TM, Blaha G, Wilson DN, Marahiel MA, Nierhaus KH. Dissection of the mechanism for the stringent factor RelA. Mol. Cell. 2002; 10: 779-788.
3. Pesavento C, Hengge R. Bacterial nucleotide-based second messengers. Curr. Opin. Microbiol. 2009; 12(2): 170-176.
4. Wu J, Long Q, Xie J. (p)ppGpp and drug resistance. J. Cell. Physiol. 2010; 224(2): 300-304.
5. Kanjee U, Ogata K, Houry WA. Direct binding targets of the stringent response alarmone (p)ppGpp. Mol. Microbiol. 2012; 85(6): 1029-1043.
6. Atkinson GC, Tenson T, Hauryliuk V. The RelA/SpoT Homolog (RSH) superfamily: Distribution and functional evolution of ppGpp synthetases and hydrolases across the tree of life. PLOS One. 2011; 6(8): 1-21.
7. Yan X, Zhao C, Budin-Verneuil A, Hartke A, Rince A, Gilmore MS, Auffray Y, Pichereau V. The (p)ppGpp synthetase RelA contributes to stress adaptation and virulence in *Enterococcus faecalis* V583. Microbiology. 2009; 155(Pt 10): 3226-3237.
8. Sajish M, Kalayil S, Verma SK, Nandicoori VK, Prakash B. The significance of EXDD and RXKD motif conservation in Rel proteins. J. Biol. Chem. 2009; 284: 9115-9123.
9. Jain V, Saleem-Batcha R, China A, Chatterji D. Molecular dissection of the mycobacterial stringent response protein Rel. Protein. Sci. 2006; 15(6): 1448-1464.
10. Wendrich TM, Blaha G, Wilson DN, Marahiel MA, Nierhaus KH. Dissection of the mechanism for the stringent factor RelA. Mol. Cell. 2002; 10: 779-788.
11. Dalebroux ZD, Svensson SL, Gaynor EC, Swanson MS. ppGpp conjures bacterial virulence. Microbiol. Mol. Biol. Rev. 2010; 74(2): 171-199.
12. Braeken K, Moris M, Daniels R, Vanderleyden J, Michiels J. New horizons for (p)ppGpp in bacterial and plant physiology. Trends. Microbiol. 2006; 14: 45-54.
13. Magnusson LU, Farewell A, Nystrom T. ppGpp: a global regulator in *Escherichia coli*. Trends. Microbiol. 2005; 13: 236-242.
14. Potrykus K and Cashel M. (p)ppGpp: still magical? Ann. Rev. Microbiol. 2008; 62: 35-51.
15. Srivatsan A and Wang JD. Control of bacterial transcription, translation and replication by (p)ppGpp. Curr. Opin. Microbiol. 2008; 11: 100-105.
16. Sajish M, Tiwari D, Rananaware D, Nandicoori VK, Prakash B. A charge reversal differentiates (p)ppGpp synthesis by monofunctional and bifunctional Rel proteins. J. Biol. Chem. 2007; 282: 34977-34983.
17. Mittenhuber G. Comparative genomics and evolution of genes encoding bacterial (p)ppGpp synthetases/hydrolases (the Rel, RelA and SpoT proteins). J. Mol. Microbiol. Biotechnol. 2001; 3(4): 585-600.
18. Mechold U and Malke H. Characterization of the stringent and relaxed responses of *Streptococcus equisimilis*. J. Bacteriol. 1997; 179: 2658-2667.
19. Mechold U, Cashel M, Steiner K, Gentry D, Malke H. Functional analysis of a *relA/spoT* gene homolog from *Streptococcus equisimilis*. J. Bacteriol. 1996; 178: 1401-1411.
20. Gropp M, Strausz Y, Gross M, Glaser G. Regulation of *Escherichia coli* RelA requires oligomerization of the C-terminal domain. J. Bacteriol. 2001; 183: 570-579.
21. Aravind L and Koonin EV. Gleaning non-trivial structural, functional and evolutionary information about proteins by iterative database searches. J. Mol. Biol. 1999; 287: 1023-1040.
22. Wolf YI, Aravind L, Grishin NV, Koonin EV. Evolution of aminoacyl-tRNA synthetases – analysis of unique domain architectures and phylogenetic trees reveals a complex history of horizontal gene transfer events. Genome. Res. 1999; 9: 689-710.
23. Krasny L and Gourse RL. An alternative strategy for bacterial ribosome synthesis: *Bacillus subtilis* rRNA transcription regulation. EMBO. J. 2004; 23: 4473-4483.
24. Primm TP, Andersen SJ, Mizrahi V, Avarbock D, Rubin H, Barry CE 3rd. The stringent response of *Mycobacterium tuberculosis* is required for long-term survival. J. Bacteriol. 2000; 182: 4889-4898.
25. Dahl JL, Kraus CN, Boshoff HI, Doan B, Foley K, Avarbock D, Kaplan G, Mizrahi V, Rubin H, Barry CE 3rd. The role of RelMtb-mediated adaptation to stationary phase in long-term persistence of *Mycobacterium tuberculosis* in mice. Proc. Natl. Acad. Sci. USA. 2003; 100: 10026-10031.
26. Taylor CM, Beresford M, Epton HAS, Sigee DC, Shama G, Andrew PW, Roberts IS. *Listeria monocytogenes relA* and hpt mutants are impaired in surface-attached growth and virulence. J. Bacteriol. 2002; 184(3): 621-628.
27. Hammer BK and Swanson MS. Co-ordination of *Legionella pneumophila* virulence with entry into stationary phase by ppGpp. Mol. Microbiol. 1999; 33: 721-731.
28. Zusman T, Gal-Mor O, Segal G. Characetrization of a *Legionella pneumophila* relA insertion mutant and roles of RelA and RpoS in virulence gene expression. J. Bacteriol. 2002; 184: 67-75.
29. Haralalka S, Nandi S, Bhadra RK. Mutation in the relA gene of *Vibrio cholerae* affects in vitro and in vivo expression of virulence factors. J. Bacteriol. 2003; 185: 4672-4682.
30. Erickson DL, Lines JL, Pesci EC, Venturi V, Storey DG. *Pseudomonas aeruginosa* relA contributes to virulence in *Drosophila melanogaster*. Infect. Immun. 2004; 72: 5638-5645.
31. Vogt SL, Green C, Stevens KM, Day B, Erickson DL, Woods DE, Storey DG. The stringent response is essential for *Pseudomonas aeruginosa* virulence in the rat lung agar bead and *Drosophila melanogaster* feeding models of infection. Infect. Immun. 2011; 79(10): 4094-4104.
32. Sun W, Roland KL, Branger CG, Kuang X, Curtiss R III. The role of *relA* and *spoT* in *Yersinia pestis* KIM5+ pathogenicity. PLOS One. 2009; 4(8): e6720. Doi: 10.1371/journal.pone.0006720.
33. Muller CM, Conejero L, Spink N, Wand ME, Bancroft GJ, Titball RW. The role of RelA and SpoT in *Burkholderia pseudomallei* virulence and immunity. Infect. Immun. 2012; 80(9): 3247-3255.
34. Pizarro-Cerda J and Tedin K. The bacterial signal molecule, ppGpp, regulates *Salmonella* virulence gene expression. Mol. Microbiol. 2004; 52: 1827-1844.
35. Dean RE, Ireland PM, Jordan JE, Titball RW, Oyston PCF. RelA regulates virulence and intracellular survival of *Francisella novicida*. Microbiology. 2009; 155: 4104-4113.
36. Gentry DR, Hernandez VJ, Nguyen LH, Jensen DB, Cashel M. Synthesis of the stationary-phase sigma factor σ^S is regulated by ppGpp. J. Bacteriol. 1993; 175: 7982-7989.
37. Boaretti M, Lleo MM, Bonato B. Involvement of rpoS in the survival of *Escherichia coli* in the viable but non-culturable state. Environ. Microbiol. 2003; 5 (10): 986-996.
38. Hulsmann A, Rosche TM, Kong I-S, Hassan HM, Beam DM, Oliver JD. RpoS- dependent stress response and exoenzyme production in *Vibrio vulnificus*. Appl. Environ. Microbiol. 2003; 69(10): 6114-6120.
39. Zhang Y. The magic bullets and tuberculosis drug targets. Ann. Rev. Pharmacol. Toxicol. 2005; 45: 529-564.
40. Hogg T, Mechold U, Malke H, Cashel M, Hilgenfeld R. Conformational antagonism between opposing active sites in a bifunctional RelA/SpoT homolog modulates (p)ppGpp metabolism during the stringent response. Cell. 2004; 117: 57-68.
41. Wexselblatt E, Katzhendler J, Saleem-Batcha R, Hansen G, Hilgenfeld R, Glaser G, Vidavski RR. ppGpp analogues inhibit syntheatse activity of Rel proteins from Gram-negative and Gram-positive bacteria. Bioorg. Med. Chem. 2010; 18: 4485-4497.

42. Wexselblatt E, Oppenheimer-Shaanan Y, Kaspy I, London N, Schueler-Furman O, Yavin E, Glaser G, Katzhendler J, Ben-Yehudaz S. Relacin, a novel antibacterial agent targeting the stringent response. PLoS Pathog. 2012; 8(9): e1002925.
43. Altschul SF, Gish W, Miller W, Myers EW, Lipman DJ. A basic local alignment search tool. J. Mol. Biol. 1990; 215: 403-410.
44. Guex N and Peitsch MC. Swiss-Model and the Swiss-PDB Viewer: An environment for comparative protein modeling. Electrophoresis. 1997; 18: 2714-2723.
45. Laskowski RA, MacArthur MW, Moss DS, Thornton JM. PROCHECK, a program to check the stereochemical quality of protein structures. J. Appl. Crystallogr. 1993; 26 (2): 283-291.
46. Sippl MJ. Recognition of errors in three-dimensional structures of proteins. Proteins. 1993; 17(4): 355-362, ISSN 0887-3585.
47. Holst MJ and Saied F. Numerical-solution of the nonlinear Poisson-Boltzmann equation-developing more robust and efficient methods. J. Comput. Chem. 1995; 16: 337-364.
48. Sanner M. Python: a programming language for software integration and development. J. Mol. Graphics. Modell. 1999; 17: 57-61.
49. Trott O and Olson A. AutoDock Vina: Improving the speed and accuracy of docking with a new scoring function, efficient optimization, and multithreading. J. Comput. Chem. 2010; 31(2): 455-461.
50. Jones MK, Warner E, Oliver JD. Survival of and In Situ Gene Expression by *Vibrio vulnificus* at Varying Salinities in Estuarine Environments. Appl. Environ. Microbiol. 2008; 74(1): 182-187.
51. Nicholas KB and Nicholas HB Jr. GeneDoc: a tool for editing and annotating multiple sequence alignments. 1997. Distributed by the author.